JOURNAL OF Materials CHEMISTRY

Crystal engineering on layered zirconium phosphonates. Crystal structure (from X-ray powder data) and non-covalent interactions on the layered zirconium compound of 4-[bis(phosphonomethyl)-amino]butanoic acid†

Riccardo Vivani,* Umberto Costantino and Morena Nocchetti

Dipartimento di Chimica, via Elce di Sotto 8, 06123 Perugia, Italy. E-mail: ric@unipg.it

Received 29th April 2002, Accepted 14th June 2002
First published as an Advance Article on the web 3rd October 2002

A new layered zirconium diphosphonate fluoride, $ZrHF(O_3PCH_2)_2NHC_3H_6CO_2$, has been prepared by the reaction of zirconyl chloride with 4-[bis(phosphonomethyl)amino]butanoic acid in the presence of HF. Its structure has been determined "*ab initio*" by X-ray powder data. It crystallizes in the monoclinic space group $P2_1/c$ (No. 14), with $a = 12.9640(3)$ Å, $b = 8.9900(4)$ Å, $c = 10.7924(4)$ Å, $\beta = 101.854(4)^\circ$, and $Z = 4$. Both of the phosphonic groups of each diphosphonate building block are bonded to zirconium atoms on the same side of the layers. Only one organic residue is associated with two phosphonate tetrahedra. The packing of layers creates an interdigitated arrangement of organic groups in the interlayer region. Two strong non-covalent interactions are present in the structure. One of them involves neighbouring P–OH and amino groups, while the other interaction engages terminal carboxylic groups and fluorine atoms belonging to adjacent layers. Thermal treatment at 240 °C causes the loss of one mole of HF per mole of zirconium, with the formation of a stable compound in which carboxylate groups probably coordinate to the zirconium atoms belonging to adjacent layers. Preliminary experiments of intercalation with ammonia and short alkylamines are also reported.

Introduction

Layered zirconium phosphates and phosphonates are the subjects of growing interest in the field of materials chemistry. They are obtained in several different layered structures, each of them corresponding to a different specific reactivity.[1–3] Often, these main structures can be modified by topotactic exchange reactions, in which a phosphate, or a phosphonate group, is replaced by another group with a different reactivity and geometry.[1,4] Zirconium phosphates and phosphonates are usually able to incorporate guest species by means of intercalation reactions carried out under mild conditions.[2] One of the most intriguing topics is the induction of an ordered distribution of free spaces, available for guest species, in the interlayer region of these compounds. In α-zirconium phosphonates of general formula $Zr(O_3PR)_2$, there are two organic R groups, pointing towards the interlayer region, for each zirconium atom.[5] The free area associated with each R group is 24 $Å^2$ and, in general, the interlayer space is filled by these organic groups, which are arranged in a compact double layer.[6] A generic phosphonate derivative of γ-zirconium phosphate has the formula $ZrPO_4[O_2P(OH)R]$. In a γ-type structure the free area associated with each R group is 36 $Å^2$,[7] and also in this case the organic groups tend to fill the interlayer region as a compact double layer.[8–10] Considerable effort has been directed towards decreasing the density of the organic groups covalently bonded to the inorganic α- and γ-layers.[11,12] Good results have been obtained either by using diphosphonate groups that can covalently join adjacent inorganic layers, or by alternating big R with small R' groups, in mixed phosphonate compounds. In some cases, by the right choice of organic group, these methodologies have led to materials showing permanent interlayer microporosity.[13–15]

A different strategy has recently been investigated in our laboratory in an effort to reduce the overcrowding of organic groups in the interlayer space, which was first pursued by Bujoli *et al.* for layered M(II) compounds.[16] This strategy consists of the use of selected diphosphonate building blocks that can connect both phosphonic groups to metal atoms on the same side of layers leading to the formation of layered compounds with half of the organic groups in the interlayer region.

This paper reports the preparation and structural characterization, by X-ray powder diffraction data, of a new layered zirconium diphosphonate containing butanoic groups. Chemical and geometric features of the diphosphonate building blocks used induced an unusual layered structure with only one organic group for each zirconium atom.

Experimental

Synthetic procedures

Reagents. $ZrOCl_2 \cdot 8H_2O$ was a Merck Pro Analysi product. All the other chemicals were Carlo Erba RPE grade.

Synthesis of the diphosphonic acid. The 4-[bis(phosphonomethyl)amino]butanoic acid, of formula $(H_2O_3PCH_2)_2NC_4H_7O_2$ (hereafter **1**), was synthesized according to the Moedritzer–Irani method.[17]

After the synthesis, the diphosphonic acid, which was obtained as a white microcrystalline solid, was purified by recrystallization using ethanol as solvent. The solid was then characterized by determination of its melting point, C, H and N elemental analysis, and X-ray powder diffraction qualitative phase analysis.

†Basis of a presentation given at Materials Discussion No. 5, 22–25 September 2002, Madrid, Spain.

 DOI: 10.1039/b204097b

Synthesis of zirconium diphosphonate. The zirconium salt of **1**, of formula $ZrHF(O_3PCH_2)_2NHC_3H_6CO_2$ (hereafter **2**) was prepared as follows: a clear solution containing 0.05 mol L^{-1} of Zr(IV), 0.1 mol L^{-1} of **1** and 0.4 mol L^{-1} of hydrofluoric acid was prepared using water as solvent. The solution (0.062 L) was maintained in a closed plastic vessel at 80 °C until a white precipitate formed. Typically, the reaction time was 24 h. The precipitate was separated by centrifugation and washed four times with water. Finally it was dried in an oven at 70 °C. The microcrystals appeared, by SEM analysis, as platelets of about 1 μm average size. Analysis, calcd. for $ZrP_2FO_8NC_6H_{12}$ (found): C, 18.08 (17.59); H, 3.01 (3.15); N, 3.52 (3.48); Zr, 22.91 (22.87); P, 15.57 (15.63); F 4.77% (4.55%).

Intercalation reactions. Intercalation reactions of **2** with ammonia and short chain *n*-alkylamines (from methyl- to butylamine) were performed by mixing 0.2 g portions of **2** with 20 mL of 1 M amine solutions, using ethanol as solvent, at room temperature, for 24 h. The intercalation compounds were then separated by centrifugation, washed with ethanol and conditioned over the corresponding amine solution saturated with urea.

Analytical procedures

The composition of **2** was determined as follows. Zirconium, phosphorus and fluorine contents were determined as ZrO_2, phosphates and fluorides, respectively, after sample mineralization. A 0.2 g portion of the sample was mixed with an excess of an equimolar Na_2CO_3 and K_2CO_3 mixture, put in a ceramic vessel and gradually heated up to 800 °C in an oven. The calcined solid was then recovered with water, filtered on paper and washed to quantitatively transfer the soluble sodium and potassium phosphates formed into the water used for washing. Phosphate and fluoride amounts in this solution of water were determined by ion chromatography. The residual filtered solid was washed with 0.1 M hydrochloric acid to dissolve the excess alkaline carbonates, then washed with water, and finally calcined to ZrO_2, which was determined gravimetrically.

The content of fluorine was also determined using an alternative method. About 0.1 g of sample was refluxed for 3 h with 10 mL of 1 M NaOH up to complete hydrolysis. After filtration and appropriate dilution, the solution was injected into the ion chromatograph.

Instrumental procedures

C, H and N elemental analysis was performed with a Carlo Erba 1106 Analyser.

Ion chromatography was performed with a Dionex series 2000 i/sp instrument, using an IonPack AS4A column and a buffer solution of the following composition as eluent: 1.7×10^{-3} M $NaHCO_3$, 1.8×10^{-3} M Na_2CO_3 (3.5×10^{-3} M for fluoride ions).

Coupled thermogravimetric (TG) and differential thermal (DTA) analyses were performed with a Netzsch STA490C thermoanalyzer under a 20 mL min^{-1} air flux at a heating rate of 5 °C min^{-1}.

X-Ray powder diffraction (XRD) patterns for structure determination and Rietveld refinement were collected according to the step scanning procedure using Cu-Kα radiation on a Philips X'PERT APD diffractometer and PW3020 goniometer equipped with a bent graphite monochromator on the diffracted beam. 0.5° divergence and scatter slits and a 0.1 mm receiving slit were used. The LFF ceramic tube operated at 40 kV and 30 mA. To minimize preferred orientations, the sample was carefully sideloaded onto an aluminium sample holder with an oriented quartz monocrystal underneath. Further acquisition details are reported in Table 1. Other XRD patterns were recorded using larger slits, a 0.03° 2θ step size and 1 s counting time in the 2–60° 2θ range.

FT-IR spectra of the solid samples were recorded under vacuum with a Bruker IFS 113 V spectrometer using KBr pellets for sample analysis.

Table 1 Crystal data and refinement details for **2**

Empirical formula	$ZrP_2FO_8NC_6H_{12}$
Formula weight	398.2
Crystal system	Monoclinic
Space group	$P2_1/c$
a/Å	12.9640(3)
b/Å	8.9900(4)
c/Å	10.7924(4)
β/degrees	101.854(4)
Volume/Å^3	1230.99(5)
Z	4
T/°C	25
Calculated density/g·cm^{-3}	2.15
Pattern range, 2θ/°	10–139
Step scan increment, 2θ/°	0.02
Step scan time/s	30
No. of data	6508
No. of reflections	2647
No. of variables	90
R_p[a]	0.076
R_{wp}[b]	0.098
R_F2[c]	0.081
χ[d]	3.17

[a] $R_p = \Sigma|I_o - I_c|/\Sigma I_o$. [b] $R_{wp} = [\Sigma w(I_o - I_c)^2/\Sigma w I_o^2]$. [c] $R_F2 = \Sigma|F_o^2 - F_c^2|/\Sigma|F_o^2|$. [d] $\chi = [\Sigma w(I_o - I_c)^2/(N_o - N_{var})]$.

Structure determination and refinement for 2

A first determination of cell parameters was made using the TREOR90 program.[18] For this, a preliminary peak-profile fitting, using pseudo-Voigt functions for the determination of the position of $K\alpha_1$ maxima, was carried out. Indexation gave the following monoclinic cell: $a = 12.987(4)$ Å, $b = 8.993(1)$ Å, $c = 10.803(2)$ Å, $\beta = 101.81(3)°$ as the best solution ($M(20) = 35$[19]). The refined unit cell parameters are reported in Table 1. The analysis of the indexed pattern clearly revealed the presence of the following limiting reflection conditions: $0k0$, $k = 2n$ and $h0l$, $l = 2n$, which suggests $P2_1/c$ as the probable space group. In addition, a systematic comparison of the number of peaks observed and the number of possible peaks, in all monoclinic space groups using the Checkcell program,[20] estimated $P2_1/c$ as the best choice.

The structure was solved by direct methods using the EXPO program,[21] by which eleven of the nineteen atoms of the asymmetric unit were detected. A series of Rietveld refinements alternated with Fourier difference maps, performed using the GSAS program,[22] revealed the positions of the remaining two oxygen atoms of the layer framework, all four carbon atoms of the alkyl chain and the two oxygen atoms of the carboxylic group.

The whole structure was then refined using the GSAS program. The scale factor, background (16 terms cosine Fourier series), zero shift, cell parameters and peak profile were first refined. The atomic parameters were then refined. All the atoms were refined isotropically and neutral atomic scattering factors were used. The thermal parameters of the heavy atoms (Zr and P) were refined independently, while those of the light atoms (F, O, N and C) were refined by constraining the program to apply the same shifts. The shape of the profile was modelled by a pseudo-Voigt function (6 parameters) in which a parameter for asymmetry at a low angle was included.[23] A March–Dollase correction[24,25] along the $h00$ direction was applied for the preferred orientation. No correction was made for absorption. Stereochemical restraints were introduced for bond distances (2.03(5) Å for Zr–O, 1.90(5) Å for Zr–F, 1.53(5) Å for P–O, 1.80(5) Å for P–C, 1.54(5) Å

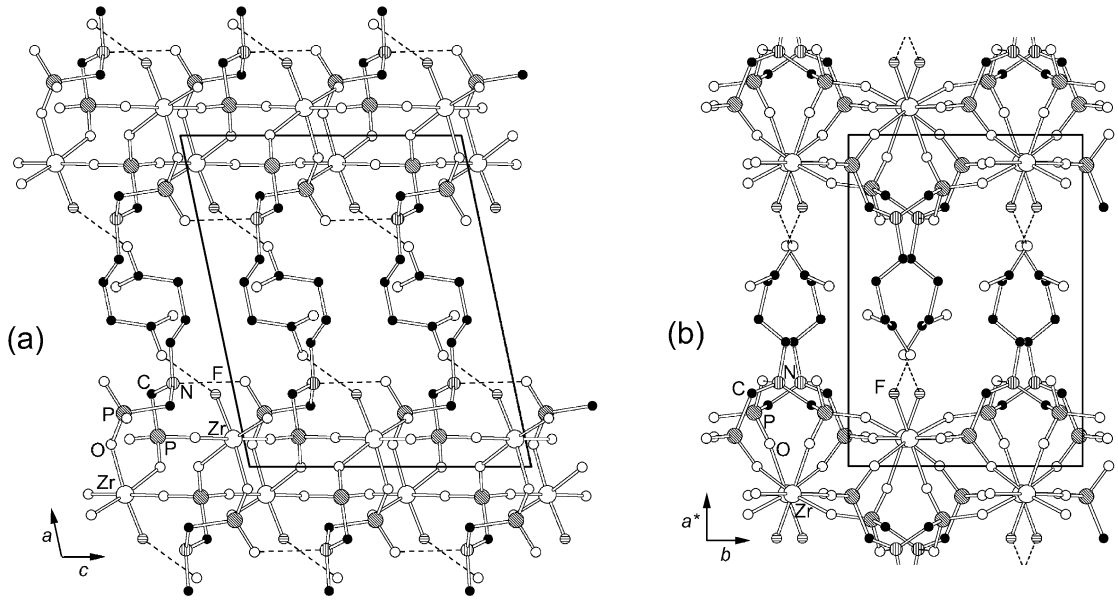

Fig. 1 (a) Ball-and-stick representation of the structure of **2** viewed along the *b* axis. (b) The same structure viewed down the *c* axis.

for C–C, 1.30(5) Å for C–O and 1.45(5) Å for C–N bonds) to avoid divergence in the first stages of refinement. The statistical weight of these restraints was decreased to a small value as the refinement proceeded, but it was not possible to set it to zero because of some unrealistic light atom bond distances. The first peak of the pattern, at about 6.9° 2θ, was excluded from the refinement because of its strong asymmetry. At the end of the refinement, the shifts in all parameters were less than their standard deviations.

Results and discussion

Structure description of 2

Fig. 1 shows the structure of **2**, while Fig. 2 shows its asymmetric unit. Table 1 lists the crystal data and refinement details, Table 2 reports the structural parameters, while Table 3 lists selected bond distances and angles for **2**. Fig. 3 shows the final Rietveld and difference plot.

The structure of **2** is composed of the packing of hybrid inorganic–organic layers. Each layer is made of ZrO_5F octahedra sharing the five corners occupied by oxygen atoms with O_3PC phosphonate tetrahedra. Pairs of these phosphonates belong to the same diphosphonate moiety and are bridged by a nitrogen atom. A butanoic group is also bonded to this nitrogen atom and points towards the interlayer region. Zirconium octahedra are positioned in two parallel planes about 2.2 Å apart. These planes are parallel to the *bc* plane, while the octahedra axis defined by F–Zr–O(8) bonds is tilted towards both the *b* and *c* directions. The zirconium atoms are coordinated by five oxygen atoms bonded to five different phosphonate groups and one fluorine atom, which occupies the most external coordination position in relation to the layer surface. Two of the five phosphonate tetrahedra, *cis*-coordinated to the zirconium, are from the same diphosphonate residue, so that each zirconium atom is coordinated to four different diphosphonates. The two phosphonate groups of each diphosphonate are crystallographically and chemically non-equivalent. One of them is located approximately in one of the zirconium planes, it shares each of its three oxygens with three different zirconium atoms, two of which belong to one zirconium plane, and the third to the other parallel plane. The

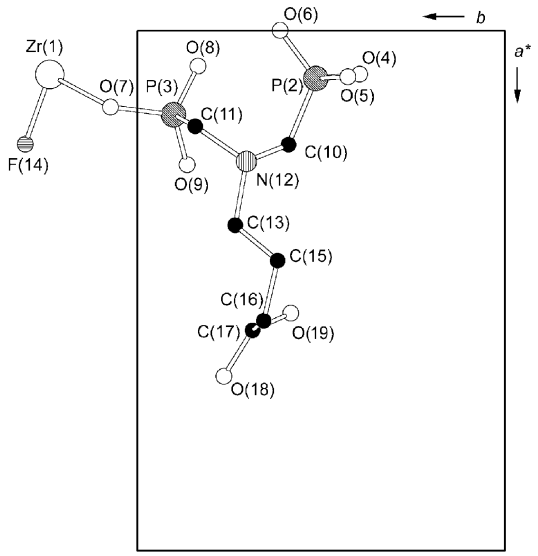

Fig. 2 Ball-and-stick representation of the asymmetric unit of **2** viewed down the *c* axis.

Table 2 Fractional atomic coordinates and isotropic thermal parameters for **2**

Atom name	*x*	*y*	*z*	$10^3 U_{iso}$
Zr(1)	0.0834(2)	−0.2376(4)	0.4629(3)	2.27(6)
P(2)	0.0910(5)	0.4829(8)	0.6981(8)	2.1(2)
P(3)	0.1612(4)	0.098(1)	0.5936(9)	4.2(2)
O(4)	0.0882(8)	0.574(1)	0.825(1)	2.0(1)
O(5)	0.0837(8)	0.606(1)	0.596(1)	2.0
O(6)	−0.0022(7)	0.388(1)	0.681(1)	2.0
O(7)	0.1443(7)	−0.075(1)	0.597(1)	2.0
O(8)	0.0679(6)	0.166(1)	0.527(1)	2.0
O(9)	0.2570(7)	0.135(2)	0.546(1)	2.0
C(10)	0.213(1)	0.415(4)	0.698(4)	2.0
C(11)	0.187(1)	0.154(2)	0.764(1)	2.0
N(12)	0.2517(8)	0.296(2)	0.789(1)	2.0
C(13)	0.3753(8)	0.268(2)	0.799(2)	2.0
F(14)	0.2159(6)	−0.304(1)	0.434(1)	2.0
C(15)	0.4424(9)	0.380(2)	0.882(2)	2.0
C(16)	0.558(1)	0.345(2)	0.882(1)	2.0
C(17)	0.578(1)	0.315(2)	0.746(1)	2.0
O(18)	0.6646(7)	0.237(2)	0.730(1)	2.0
O(19)	0.5420(7)	0.416(2)	0.656(1)	2.0

Table 3 Selected bond lengths and angles for **2**

Bond	Length/Å	Bond angle	Angle/degrees
Zr(1)–O(4)	2.10(1)	O(4)–Zr(1)–O(5)	178.2(4)
Zr(1)–O(5)	2.01(1)	O(4)–Zr(1)–O(6)	90.7(5)
Zr(1)–O(6)	2.16(1)	O(4)–Zr(1)–O(7)	86.3(4)
Zr(1)–O(7)	2.10(1)	O(4)–Zr(1)–O(8)	89.2(4)
Zr(1)–O(8)	2.09(1)	O(4)–Zr(1)–F(14)	86.9(4)
Zr(1)–F(14)	1.91(1)	O(5)–Zr(1)–O(6)	90.3(4)
P(2)–O(4)	1.60(1)	O(5)–Zr(1)–O(7)	92.9(5)
P(2)–O(5)	1.56(1)	O(5)–Zr(1)–O(8)	92.3(4)
P(2)–O(6)	1.46(1)	O(5)–Zr(1)–F(14)	91.6(5)
P(2)–C(10)	1.70(2)	O(6)–Zr(1)–O(7)	172.4(5)
P(3)–O(7)	1.57(1)	O(6)–Zr(1)–O(8)	84.5(4)
P(3)–O(8)	1.42(1)	O(6)–Zr(1)–F(14)	90.5(4)
P(3)–O(9)	1.47(1)	O(7)–Zr(1)–O(8)	88.4(4)
P(3)–C(11)	1.87(1)	O(7)–Zr(1)–F(14)	96.3(4)
N(12)–C(10)	1.47(4)	O(8)–Zr(1)–F(14)	173.7(5)
N(12)–C(11)	1.52(1)	O(4)–P(2)–O(5)	103.7(8)
N(12)–C(13)	1.60(1)	O(4)–P(2)–O(6)	104.2(7)
C(13)–C(15)	1.50(2)	O(4)–P(2)–C(10)	112(1)
C(15)–C(16)	1.54(1)	O(5)–P(2)–O(6)	113.6(8)
C(16)–C(17)	1.56(1)	O(5)–P(2)–C(10)	100.1(9)
C(17)–O(18)	1.36(1)	O(6)–P(2)–C(10)	122.4(9)
C(17)–O(19)	1.34(1)	O(7)–P(3)–O(8)	109.4(7)
		O(7)–P(3)–O(9)	111.2(9)
O(9)···N(12)	2.83(2)	O(7)–P(3)–C(11)	103.9(8)
O(18)···F(14)	2.65(2)	O(8)–P(3)–O(9)	114.9(9)
		O(8)–P(3)–C(11)	110.3(8)
		O(9)–P(3)–C(11)	106.7(7)
		P(2)–C(10)–N(12)	117(1)
		P(3)–C(11)–N(12)	113(1)
		C(10)–N(12)–C(11)	113(1)
		C(10)–N(12)–C(13)	111(1)
		C(11)–N(12)–C(13)	113(1)
		N(12)–C(13)–C(15)	112(1)
		C(13)–C(15)–C(16)	108(1)
		C(15)–C(16)–C(17)	113(1)
		C(16)–C(17)–O(18)	121(1)
		C(16)–C(17)–O(19)	118(1)
		O(18)–C(17)–O(19)	115.2(9)

other phosphonate group is bonded to only two zirconium atoms which belong to two different zirconium planes. The remaining P–OH group points towards the aminic nitrogen atom belonging to the nearest adjacent diphosphonate group on the same side of the layer. The PO···N distance is 2.83 Å, indicating that a hydrogen bond is present between the two atoms. It is very likely that the amino group is protonated by the phosphonate. We were not able to detect the position of the hydrogen between the N and O atoms by our diffraction data, however, recent reports in the literature of single crystal X-ray structural data on similar systems,[26,27] strongly support the hypothesis that the nitrogen atom is protonated by the acidic phosphonate group and therefore the system has a zwitterionic character. This hypothesis is also supported by the presence, in the IR absorption spectrum, of several superimposed bands of

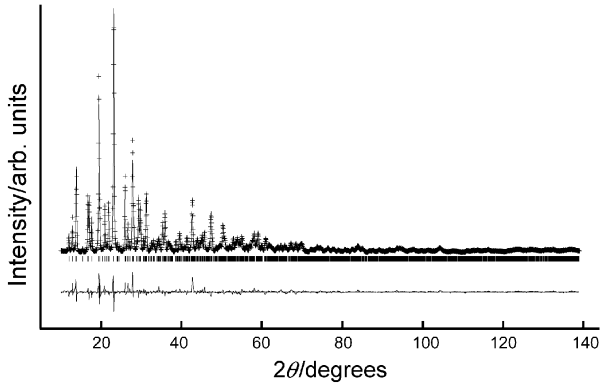

Fig. 3 Final Rietveld and difference plot for **2**.

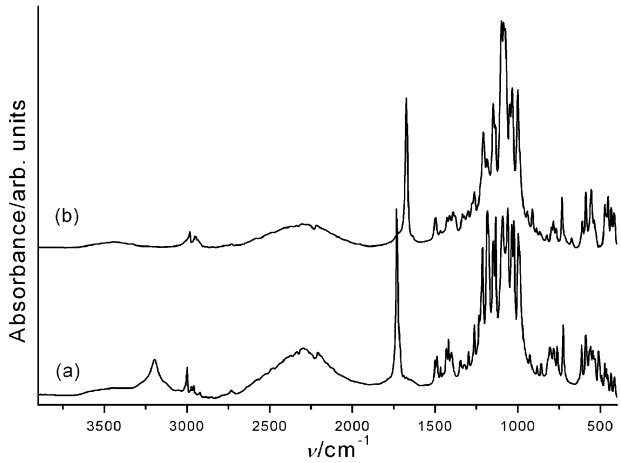

Fig. 4 FT-IR absorption spectrum of **2** as prepared (a) and after heating at 240 °C for 1 h (b).

medium intensity in the range 2600–2200 cm^{-1}, which are characteristic of $R_3N–H^+$ vibrations (Fig. 4, curve (a)). This aspect will be discussed in more detail later on.

Butanoic residues are bonded to nitrogen atoms on both sides of the inorganic layers and project into the interlamellar space. The first three carbon atoms of this group are close to their fully extended *trans* conformation (N(12)–C(13)–C(15)–C(16) torsion angle = 178.5°), while the rest of the alkyl chain is in a *gauche* conformation, since the torsion angle between the nitrogen atom of the amino group and the carboxylic carbon atom (C(13)–C(15)–C(16)–C(17) torsion angle) is 46.5°. In this structure the free area associated with each organic pendant group is 48.6 $Å^2$, a large value if compared with those of α- and γ-type structures (24.0 and 35.7 $Å^2$, respectively). This value is more than twice the estimated van der Waals cross-section of an alkyl chain (18.6 $Å^2$).[28] Due to this, the packing of the layers generates an unusual interdigitated arrangement of organic groups coming from adjacent layers. One of the terminal carboxylic oxygen atoms of the butanoic group, O(18), has a strong interaction with a fluorine atom bonded to the adjacent layer, evidenced by the F(14)···O(18) distance of only 2.65 Å. The hydrogen atom between F and O could not be unequivocally located from our data. The IR absorption spectrum (Fig. 4, curve (a)) shows a strong and sharp band at 3197 cm^{-1}, that can be ascribed either to $ZrF–H^+$, or to COO–H stretching vibrations. We favour the first suggestion, because O–H stretching bands of carboxylic acid groups are generally broader than those found experimentally when these groups are involved in strong hydrogen bonding.[29] Comparison of IR spectra before and after heating the sample at 240 °C, the temperature at which HF is lost, seems to further support this suggestion. However, neither option can be excluded at the moment.

Thermal behaviour

Fig. 5 shows the TG and DTA curves for **2**. Weight starts to be lost at about 180 °C. The TG curve shows an initial well-defined step in the range 180–280 °C, after which a plateau is reached, indicating that a stable compound has been formed. During this transformation, the compound loses 5.0% of its initial weight, corresponding to the loss of one mole of HF per mole of zirconium, as confirmed by chemical analysis of the sample after heating at 240 °C for 1 h. The resulting compound had the following composition: $Zr(O_3PCH_2)_2NHC_3H_6CO_2$. Fig. 6 shows a comparison of the XRD patterns before and after this thermal treatment. Other than the decrease in the interlayer distance from 12.7 to 11.9 Å, after heating the whole pattern shows small changes. Unfortunately, our attempts to refine the structure of this compound by the Rietveld method

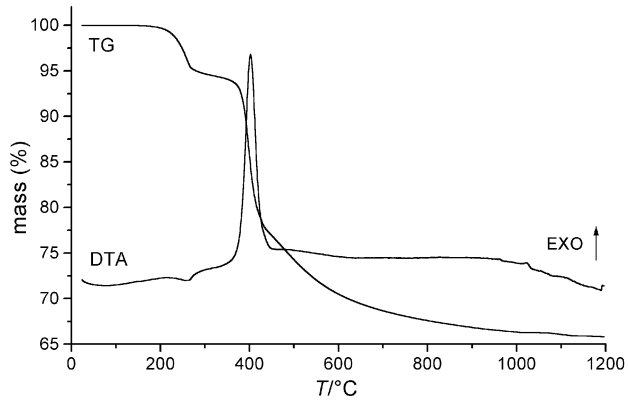

Fig. 5 TG and DTA curves for **2**.

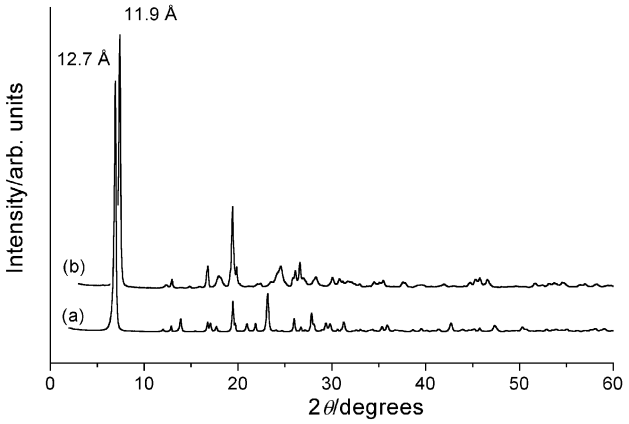

Fig. 6 XRD patterns of **2** before (a) and after thermal treatment at 240°C for 1 h (b).

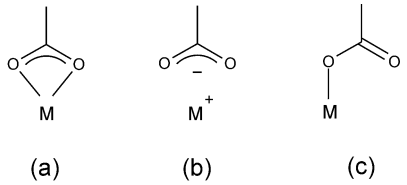

Fig. 7 Possible interactions between anionic carboxylate groups and unsaturated metal cations.

using these data were unsuccessful because of the global loss of crystallinity. However, these data (together with the information coming from the IR vibrational spectra of **2** before and after heating, will be discussed in the next section) can be interpreted on the basis of the breaking Zr–F bonds and the loss of HF groups, which leaves positively charged zirconium atoms in the inorganic layer. Also due to the decrease in the interlayer distance, we can assume that carboxylate anions will coordinate to the unsaturated metals as bidentate ligands (Fig. 7(a)), or will have ionic interactions with the positive metal centres (Fig. 7(b)). Both (a) and (b) conditions should lead to a decrease in the C–O bond order, and therefore, to a decrease in the IR absorption frequency of the C=O group,[30] as observed in the IR spectrum (Fig. 4). The two situations can be represented as shown in Fig. 8.

In contrast, coordination of the carboxylate group to the metal cation as a monodentate ligand (Fig. 7(c)) should shift the C=O absorption band to higher frequencies,[30] and therefore it is less probable. However, in the absence of accurate structural data, it is not possible to definitely reject any of these possibilities.

The organic part of **2** begins to oxidize and/or decompose at about 360 °C. At the end of the TG analysis, at 1200 °C, only cubic ZrP_2O_7 was found. The total weight loss is 34.1%, in good agreement with the calculated value (33.4%).

FT-IR spectra

The FT-IR spectrum of **2** as prepared (Fig. 4, curve (a)), shows a strong and sharp band at 3197 cm^{-1}, which may be assigned to the ZrF–H^+ stretching vibration, with the hydrogen atom involved in a hydrogen bond with an oxygen atom of a carboxylate group. No free O–H bonds should be present because of the absence of sharp bands over 3500 cm^{-1}. The C–H stretching vibration bands are very evident near 3000 cm^{-1}. The large band in the region 2600–2200 cm^{-1} may be due to R_3N–H^+ stretching vibrations. The strong and sharp band at 1734 cm^{-1} is assigned to the antisymmetric C=O stretching vibration mode of the carboxylic group, while the complex system of bands in the region 1500–400 cm^{-1} is due to the vibrations of the rest of the framework, especially P–O stretching and bending modes.

Fig. 4, curve (b), shows the FT-IR spectrum of **2** after heating at 240°C and the consequent loss of HF. Major changes are the total absence of the strong band at 3197 cm^{-1}, supporting the hypothesis that this band is due to the ZrF–H^+ vibration, and the shift to lower energy of the strong band due to C=O antisymmetric stretching, which moves from 1734 to 1674 cm^{-1}. The interaction of carboxylate groups with metal atoms after the loss of HF, as schematically shown in Fig. 7(a) and (b), can explain the shift of this absorption band to a lower frequency,[28] as already discussed. The broad bands in the range 2600–2200 cm^{-1}, assigned to the R_3N–H^+ stretching vibrations, are still present after heating, and the complex system of absorptions from 1500 to 400 cm^{-1}, that can be attributed to the rest of the structure, is very similar to that of the original sample. These observations indicate that the structure of the

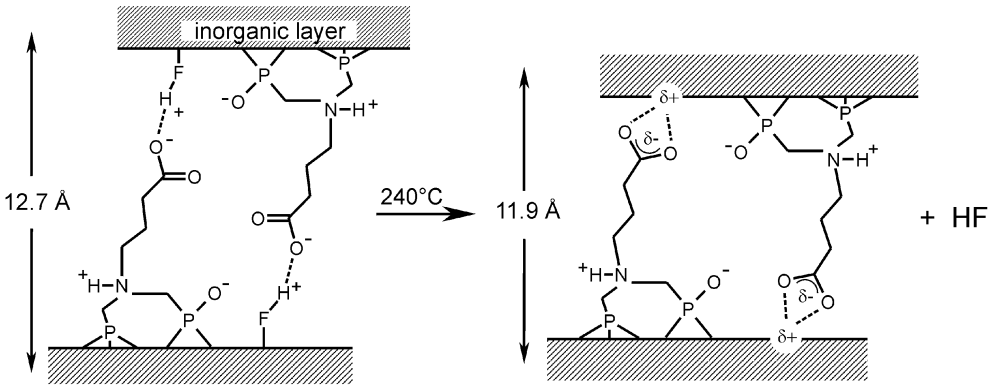

Fig. 8 Scheme of the transformation of **2** after heating at 240 °C. The zirconium–carboxylate interaction is represented as intermediate between an ionic interaction and a coordination bond.

framework does not change significantly after the loss of the HF groups.

Discussion

This new compound **2** confirms the strong tendency of zirconium to form covalent layered structures with phosphonate groups. In this case, chemical and geometric features of the diphosphonate building block used have generated a new type of layered structure. The distance between the phosphorus atoms in each pair of phosphonate groups connected to the same N atom is 3.81 Å. This value is too small for the formation of an α-type layered structure, in which the minimum distance between adjacent phosphorus atoms is about 5 Å. Furthermore, the characteristic P–O···N interaction of this diphosphonate moiety tends to exclude one of the P–O groups from coordination with zirconium, with the consequent insertion of an additional anionic ligand, F^- in this case, to complete zirconium valence and coordination.

In a recent investigation,[31] we prepared a series of layered zirconium diphosphonates using *N*,*N*-bis(phosphonomethyl)-alkylamines as organic building blocks. The structure of one of them, of formula $ZrF(O_3PCH_2)_2NHC_5H_{11}$, was solved "*ab initio*" by X-ray powder data, and was found to be closely related to that described here. The same main structural features were found. Owing to P–O···N interactions the diphosphonate groups had a zwitterionic character, and alkyl pendant groups were interdigitated in the interlayer region. However, no hydrogen bonds were present between adjacent layers due to the non-polar nature of the interlayer organic residues. The interaction between lamellae was therefore of van der Waals type.

A comparison in terms of interlayer organic group density between the structure under investigation and two other examples of layered zirconium phosphonates having different structures and containing carboxylic groups is interesting. The first example is the series of α-zirconium carboxyalkylphosphonates, of formula α-$Zr(O_3PC_nH_{2n}COOH)_2$,[32] and the second is a layered zirconium compound containing phosphate groups and *N*-(phosphonomethyl)iminodiacetic acid groups.[33] In both cases, and different from the present compound, the packing of lamellae generates a bilayer of facing carboxylic groups, interacting with each other through hydrogen bonds in the interlayer region. In α-zirconium carboxyalkylphosphonates the available free area for each pendant organic group, 24 $Å^2$, approximately fits the dimensions of this group. In the second example, phosphonate pendant groups are more spaced on the surface of the layers, with a free area of about 52 $Å^2$. This is caused by the presence of phosphate groups that alternate with phosphonate groups in the inorganic framework, and act as spacers. However, two acetic groups for each phosphonate are present; the free area for each organic group is therefore reduced to half of its value and is very similar to the previous case. In our structure there are about 49 $Å^2$ for each diphosphonate organic group. This space is doubly occupied by two butanoic groups from adjacent layers. The formation of strong interactions between the terminal carboxylic groups and fluorine atoms bonded to the adjacent layers probably favour this arrangement. Also in this case, the free area associated with each carboxylic group is 24–25 $Å^2$. However, the whole space could be recovered when using for the synthesis, diphosphonic acids with a large functional group, or when this material acts as a host for suitable species.

Intercalation reactions

Preliminary experiments have shown that **2** is able to intercalate ammonia and short *n*-alkylamines from ethanol solutions with the formation of compounds with an increased interlayer distance, depending on the length of the intercalated amine, as shown in Fig. 9. When these intercalation compounds are put in water, they spontaneously exfoliate, and stable colloidal dispersions are obtained. Colloidal dispersions are also obtained when the above intercalation reactions are carried out using amine–water solutions. This phenomenon may be due to the interposition of a guest species between the carboxylic groups and fluorine atoms, with the consequent breaking of COO···F interactions between adjacent layers. This feature discloses the intriguing potential of **2** for application in materials chemistry. For example, by using these dispersions large functional species could be intercalated and thin oriented films could be easily prepared. Further experiments are in progress to investigate the intercalation properties of this compound in more depth.

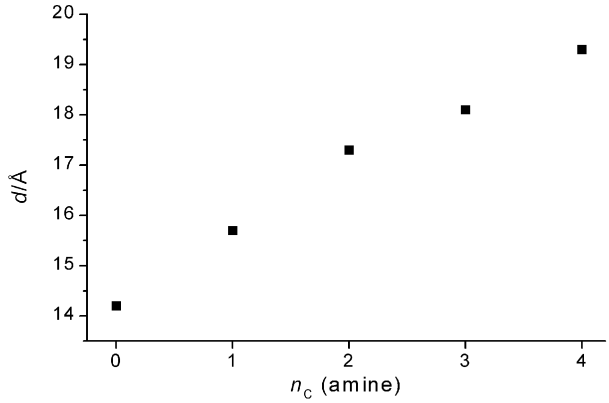

Fig. 9 Interlayer distance, *d*, of intercalation compounds of **2** with ammonia and *n*-alkylamines as a function of the number of carbon atoms in the amine alkyl chain, n_C.

Conclusions

A new layered zirconium diphosphonate has been prepared; its structure has been determined "*ab initio*" from X-ray powder data. It shows some unusual and interesting features. The layer framework is different from those of known layered zirconium phosphates and phosphonates. The packing of layers creates an interdigitated arrangement of organic groups in the interlamellar region. The presence of only one organic residue per zirconium, as well as the large free area potentially available to each of these groups, make these compounds very interesting for incorporating functional species with selected properties, by means of intercalation reactions and/or by varying the dimensions and reactivity of the organic groups bonded to the layers. Recent investigations, that will be reported elsewhere, have shown that zirconium diphosphonates of similar structure can be easily prepared using *N*,*N*-diphosphonoamines with aryl, alkyl or sulfonic functional groups.

References

1 G. Alberti, in *Comprehensive Supramolecular Chemistry*, ed. G. Alberti and T. Bein, Pergamon Press, Oxford, 1996, vol. 7, Chap. 5.
2 A. Clearfield and U. Costantino, in *Comprehensive Supramolecular Chemistry*, ed. G. Alberti and T. Bein, Pergamon Press, Oxford, 1996, vol. 7, Chap. 4.
3 A. Clearfield, in *Progress in Inorganic Chemistry*; ed. K. D. Karlin, John Wiley & Sons, New York, 1998, vol. 47, pp. 374–510.
4 G. Alberti, M. Casciola, U. Costantino and R. Vivani, *Adv. Mater.*, 1996, **8**, 291.
5 G. Alberti, U. Costantino, S. Allulli and N. Tomassini, *J. Inorg. Nucl. Chem.*, 1978, **40**, 1113.
6 D. M. Poojary, H. L. Hu, F. L. Campbell III and A. Clearfield, *Acta Crystallogr., Sect. B*, 1993, **49**, 996.
7 D. M. Poojary, B. Shpeizer and A. Clearfield, *J. Chem. Soc., Dalton Trans.*, 1995, 111.

8 G. Alberti, M. Casciola, R. Vivani and R. K. Biswas, *Inorg. Chem.*, 1993, **32**, 4600.
9 G. Alberti, R. Vivani, R. K. Biswas and S. Murcia-Mascarós, *React. Polym.*, 1993, **19**, 1.
10 G. Alberti, L. Boccali, C. Dionigi, R. Vivani, V. I. Kalchenko and L. I. Atamas, *Supramol. Chem.*, 1996, **7**, 129.
11 M. B. Dines, R. E. Cooksey, P. C. Griffith and R. H. Lane, *Inorg. Chem.*, 1983, **22**, 1003.
12 A. Clearfield, *Design of New Materials*; ed. D. L. Cocke and A. Clearfield, Plenum Press, New York, 1987.
13 G. Alberti, U. Costantino, R. Vivani and P. Zappelli, *Angew. Chem., Int. Ed. Engl.*, 1993, **32**, 1357.
14 G. Alberti, F. Marmottini, S. Murcia Mascarós and R. Vivani, *Angew. Chem., Int. Ed. Engl.*, 1994, **33**, 1594.
15 H. Byrd, K. P. Reis, M. D. Poojary, A. Clearfield and M. E. Thompson, *Chem. Mater.*, 1996, **8**, 2239.
16 V. Penicaud, D. Massiot, G. Gelbard, F. Odobel and B. Bujoli, *J. Mol. Struct.*, 1998, **31**, 470.
17 K. Moedritzer and A. Irani, *J. Org. Chem.*, 1966, **31**, 1603.
18 P. E. Werner, L. Eriksson and M. Westdhal, *J. Appl. Crystallogr.*, 1985, **18**, 367.
19 P. M. de Wolff, *J. Appl. Crystallogr.*, 1968, **1**, 108.
20 J. Laugier and B. Bochu, *LMGP-Suite*, ENSP/Laboratoire des Matériaux et du Génie Physique, BP 46, 38042 Saint Martin d'Hères, France.
21 A. Altomare, M. C. Burla, G. Cascarano, C. Giacovazzo, A. Guagliardi, A. G. G. Moliterni and G. Polidori, *J. Appl. Crystallogr.*, 1995, **28**, 842.
22 A. Larson and R. B. Von Dreele, *GSAS, Generalized Structure Analysis System*, Los Alamos National Laboratory, 1988.
23 P. Thompson, D. E. Cox and J. B. Hastings, *J. Appl. Crystallogr.*, 1987, **20**, 79.
24 A. March, *Zeit. Kristallogr.*, 1932, **81**, 285.
25 W. A. Dollase, *J. Appl. Crystallogr.*, 1986, **19**, 267.
26 A. Clearfield, C. V. K. Sharma and B. Zhang, *Chem. Mater.*, 2001, **13**, 3099.
27 J. Mao, Z. Wang and A. Clearfield, *Inorg. Chem.*, 2002, **41**, 2334.
28 A. I. Kitaigorodsky, in *Molecular Crystals and Molecules*, ed. E. M. Loebl, Academic Press, New York, 1973, p. 61.
29 B. Zhang, D. M. Poojary and A. Clearfield, *Chem. Mater.*, 1996, **8**, 1333.
30 K. Nakamoto, I*nfrared spectra of inorganic and coordination compounds*, John Wiley & Sons, New York, 1963.
31 U. Costantino, M. Nocchetti and R. Vivani, *J. Am. Chem. Soc.,* in press.
32 G. Alberti, M. Casciola, U. Costantino, A. Peraio and R. Vivani, *Solid State Ionics*, 1991, **46**, 61.
33 D. M. Poojary, B. Zhang and A. Clearfield, *Angew. Chem., Int. Ed. Engl.*, 1994, **33**, 2324.